

Real-Time Kinetics of Surfactant Molecule Transfer between Emulsion Particles Probed by in Situ Second Harmonic Generation Spectroscopy

YuMeng You,[†] Aaron Bloomfield,[†] Jian Liu, Li Fu, Seth B. Herzon,* and Elsa C. Y. Yan*

Department of Chemistry, Yale University, 225 Prospect Street, New Haven, Connecticut 06520, United States

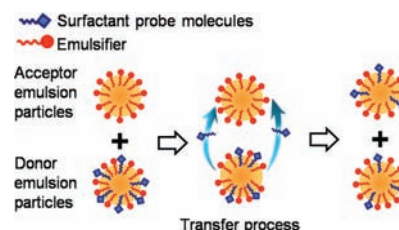
S Supporting Information

ABSTRACT: Emulsions are widely used in industrial and environmental remediation applications. The breaking and reformulation of emulsions, which occur during their use, lead to changes in their surface composition as well as their physical and chemical properties. Hence, a fundamental understanding of the transfer of surfactant molecules between emulsion particles is required for optimization of their applications. However, such an understanding remains elusive because of the lack of in situ and real-time surface-specific techniques. To address this, we designed and synthesized the surfactant probe molecules MG-butyl-1 (2) and MG-octyl-1 (3), which contain an *n*-butyl and an *n*-octyl chain, respectively, and a charged headgroup similar to that in malachite green (MG, 1). MG is known to be effective in generating second harmonic generation (SHG) signals when adsorbed onto surfaces of colloidal microparticles. Making use of the coherent nature of SHG, we monitored in real-time the transfer of 2 and 3 between oil-in-water emulsion particles with diameters of ~ 220 nm. We found that 3 is transferred ~ 600 times slower than 2, suggesting that an increase in the hydrophobic chain length decreases the transfer rate. Our results show that SHG combined with molecular design and synthesis of surfactant probe molecules can be used to measure the rate of surfactant transfer between emulsion particles. This method provides an experimental framework for examining the factors controlling the kinetics of surfactant transfer between emulsion particles, which cannot be readily investigated in situ and in real-time using conventional methods.

Emulsions are mixtures of two immiscible liquids, commonly oil droplets in water or water droplets in oil. They are often stabilized at their interfaces by surfactants. Emulsions are widely used in industrial and environmental remediation applications, including oil recovery and transport,^{1,2} emulsion polymerization,^{3,4} drug delivery,⁵ food processing, production of cosmetics, water purification,^{6,7} and cleaning up oil spills.⁸ During these processes, the emulsion droplets are broken and reformed constantly, and the surfactant molecules undergo continuous reorganization and are rapidly transferred between emulsion droplets. Because of the large surface-to-volume ratio of emulsion droplets, such variations lead to significant changes in the physical and chemical properties of emulsions.⁹ Consequently, an understanding of the fundamental factors governing the kinetics of surfactant molecule transfer between emulsion particles is critical to the development of surfactant molecules and emulsion systems.

Probing the kinetics of surfactant molecule transfer between emulsion particles (Scheme 1) in situ and in real time has been challenging. This is primarily due to the lack of surface-sensitive techniques that can isolate the signal of interfacial molecules from the signal of molecules in the bulk solution. To date, no real-time in situ kinetic study of surfactant molecule transfer between colloidal emulsion particles has been reported. The mass transport of emulsion particles to dispersed phases has been studied by NMR and fluorescence microscopy,¹⁰ and surfactant molecule transport from bulk phases to the surfaces of millimeter-sized emulsion droplets has been probed by real-time measurements of surface tension.¹¹ However, these studies

Scheme 1. Transfer of Surfactant Molecules from a Donor Emulsion Droplet to an Acceptor Emulsion Droplet



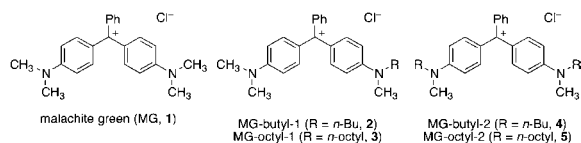
do not directly probe transfer of surfactant molecules between colloidal emulsion particles.

In this work, we approached this problem using second harmonic generation (SHG) spectroscopy combined with molecular design and synthesis. The surfactant probe (SP) molecules MG-butyl-1 (2) and MG-octyl-1 (3) (Scheme 2) were synthesized in two steps by amination¹² of di-(*p*-bromophenyl)phenylmethane followed by hydride abstraction [see the Supporting Information (SI)]. These surfactants contain an *n*-butyl and an *n*-octyl chain, respectively, and a common cationic headgroup similar to that found in malachite green (MG, 1). MG itself is known to be effective in generating SHG signals from the surfaces of colloidal microparticles using fundamental light at 800 nm. Making use of the coherent

Received: November 7, 2011

Published: February 17, 2012

Scheme 2. Structures of Surfactant Probe Molecules



nature of SHG, we measured the rates of transfer of 2 and 3 between oil-in-water emulsion droplets.

SHG, which is similar to sum-frequency generation (SFG), is a second-order surface-specific process (see the SI).¹³ Both SHG and SFG have been applied to the study of oil–water interfaces.¹⁴ The surface sensitivity originates from the selection rule that second-order optical processes are forbidden in centrosymmetric media but allowed in non-centrosymmetric media under the dipole approximation.¹³ In bulk media, molecules are randomly oriented and centrosymmetry is preserved; thus, no SHG signal is generated. In contrast, because of the asymmetric forces across interfaces, molecules at interfaces are aligned, thereby breaking the centrosymmetry. Thus, the second-order polarization, $P^{(2)}$, induced at interfaces can add up coherently and generate SHG signals:

$$E_{2\omega} \propto P^{(2)} \propto \chi^{(2)} E_{\omega} E_{\omega} \quad (1)$$

where E_{ω} is the incident field, $E_{2\omega}$ is the second-harmonic (SH) field, and $\chi^{(2)}$ is the second-order susceptibility, which is related to the microscopic second-order polarizability $\alpha^{(2)}$ by

$$\chi^{(2)} = N \langle \alpha^{(2)} \rangle \quad (2)$$

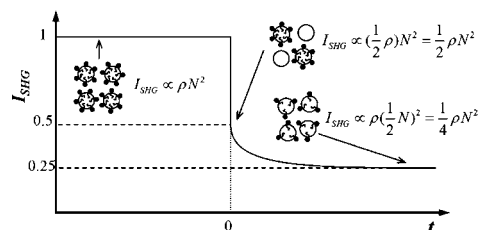
where N is the surface population and the brackets indicate an average over all molecular orientations. $\alpha^{(2)}$ is related to the properties of the interfacial molecules. The SHG signal is enhanced when the fundamental (ω) or SH frequency (2ω) coincides with an electronic transition of the molecule.

Both SHG and SFG have been extended to the study of colloidal surfaces.¹⁵ Although a colloidal particle is centrosymmetric, if the size of the particles is in the micrometer or submicrometer range, the second-order optical field generated at the particle surface can add up coherently and give a signal.^{15e} Hence, the coherent SHG signal observed from particle surfaces is different from incoherent hyper-Rayleigh scattering, which is due to fluctuations in the molecular orientation and density in isotropic bulk solutions.^{13e,15f} More discussion about the coherent addition of the SH field generated from microparticle surfaces can be found in the SI, while quantitative descriptions of SH scattering from particle surfaces have been derived in excellent theoretical studies.¹⁶ In terms of experiments, SHG and SFG have already been used to study various colloidal systems, including silica particles,^{15a–c} polymer particles,^{15d–j} carbon black particles,^{15k} droplets,^{15l} emulsions,^{15f,m,n} clay particles,^{15o} and liposomes,^{15p–r} to obtain surface populations, adsorption free energies, surface potentials, and transport properties.

Our method for probing surfactant molecule transfer between emulsion particles uses the coherent nature of the SHG signal.¹⁷ Since $I_{\text{SHG}} = |E_{2\omega}|^2$, I_{SHG} is directly proportional to the square of the surface population (N^2) if surfactant molecules are distributed evenly on the particle surfaces. When the average separation between the particles is much longer than the coherence length, the SH electric fields ($E_{2\omega}$) generated from individual particles add incoherently. Thus,

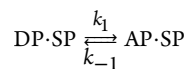
I_{SHG} also scales linearly with the particle density (ρ), so $I_{\text{SHG}} \propto \rho N^2$.

To illustrate how SHG can be used to study surfactant transfer between emulsion particles, we consider the following experiment (Scheme 3). At time $t < 0$, the sample contains a

Scheme 3. SHG Kinetic Measurement of Surfactant Molecule Transfer between Emulsion Particles: Time Dependence of I_{SHG} upon Addition of APs to DPs at $t = 0$ 

mixture of emulsion and SPs. If the SP has a UV–vis absorption in resonance with the SH frequency, it provides a strong SHG signal. The SHG intensity can be expressed as ρN^2 , where ρ is the particle density and N is the surface population of SPs on the donor emulsion particles (DPs). At $t = 0$, an equal volume of plain emulsion particles, termed acceptor particles (APs), at the same particle density is injected into the DP sample. Although the overall particle density stays the same, the density of DPs is halved. Hence, I_{SHG} becomes $\rho N^2/2$. For $t > 0$, SPs start to be transferred from DPs to APs, and I_{SHG} decays until a new equilibrium is established. When the SP concentration is low, one can assume that all SPs adsorb onto the particle surface during the transfer process, and SPs in the bulk solution can be neglected. Consequently, the SP molecules are equally distributed onto APs and DPs at equilibrium. Because the APs and DPs are now indistinguishable, the particle density is again equal to ρ , but the surface population is reduced to $N/2$. Hence, I_{SHG} becomes $\rho N^2/4$. Therefore, when the SP concentration is low and the particle separation is large, one can use SHG to observe the transfer of SPs directly.

To analyze the time-dependent I_{SHG} , we can consider the following simple model:



where DP·SP and AP·SP represent SPs adsorbed on DPs and APs, respectively. Since DPs and APs are emulsion particles of the same kind, k_1 and k_{-1} are equal (i.e., $k_1 = k_{-1} = k$). If the SP concentration is low, meaning that nearly all of the SPs are adsorbed onto DPs or APs and the bulk concentration of SPs can be ignored, the transfer rate can be written as

$$\frac{dN_{\text{AP}}}{dt} = k(N_{\text{DP}} - N_{\text{AP}}) = k(N_0 - 2N_{\text{AP}}) \quad (3)$$

where N_{DP} and N_{AP} are the numbers of SPs per DP and AP, respectively, and N_0 is the total number of SPs per DP for time $t \leq 0$. Solving eq 3 gives

$$N_{\text{AP}} = \frac{1}{2} N_0 (1 - e^{-2kt})$$

which allows $I_{\text{SHG}}(t)$ to be written as

$$I_{\text{SHG}}(t) = \frac{\rho}{2} N_{\text{AP}}^2 + \frac{\rho}{2} N_{\text{DP}}^2 = \frac{\rho}{4} N_0^2 (1 + e^{-4kt})$$

The normalized $I_{\text{SHG}}(t)$ then becomes

$$\frac{I_{\text{SHG}}(t)}{I_{\text{SHG}}(t < 0)} = \frac{1}{4}(1 + e^{-4kt}) \quad (4)$$

Equation 4 can be used to fit the decay of $I_{\text{SHG}}(t)$ as shown in Scheme 3 to obtain the rate constant, k .

To perform the kinetic measurements, we had to synthesize the SP molecules. The surfactant probes MG-butyl-1 (2) and MG-octyl-1 (3), were prepared by Buchwald–Hartwig coupling¹² of 4,4'-dibromotriphenylmethane with equimolar dimethylamine/methylbutylamine and dimethylamine/methyloctylamine mixtures, respectively. Statistical mixtures of products were formed and then separated by flash-column chromatography. 4-Dimethylamino-4'-methylbutylaminotriphenylmethane and 4-dimethylamino-4'-methyloctylaminotriphenylmethane were oxidized by treatment with ceric ammonium nitrate and HCl to afford 2 and 3, respectively. Also obtained by this sequence were dibutylated MG-butyl-2 (4) and dioctylated MG-octyl-2 (5). In this study, we only used the products containing one alkyl chain. They were characterized by standard spectroscopic techniques (see the SI). Figure 1 shows that the UV–vis spectra of 1–3 were similar, consistent with the presence of similar cationic head groups.

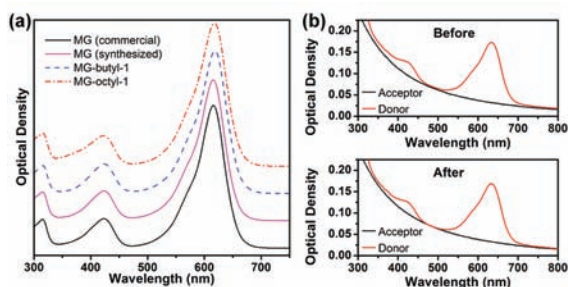


Figure 1. (a) UV–vis absorption spectra of synthesized 1–3 and commercially available 1, normalized to the absorption at ~ 620 nm. (b) UV–vis absorption spectra of DPs containing 3 (red) and APs (black). The particle density was $1.3 \times 10^{10} \text{ cm}^{-3}$, and the concentration of 3 was $2.3 \mu\text{M}$.

We prepared an oil-in-water emulsion by ultrasonication of a 1:9 (v/v) mixture of 5 mM 1-dodecanol/*n*-tetradecane solution and 5 mM sodium dodecyl sulfate/water solution, as described in the SI. The pH of both the DP and AP solutions was maintained by a buffer (1 mM phosphate, pH 6.2). Dynamic light scattering (DLS) (532 nm, ALV-5000, Langen) was used to measure the size of the emulsion, yielding an average

diameter of 226 ± 32 nm. From this we calculated the particle density used in the SHG experiments as $1.3 \times 10^{10} \text{ cm}^{-3}$, giving an average particle separation of $\sim 4 \mu\text{m}$.

To obtain the kinetic data as shown in Scheme 3, 2 or 3 was first dissolved in water at pH 4, as adjusted by HCl(aq), and diluted with the emulsion sample in the phosphate buffer to a SP concentration of $2.3 \mu\text{M}$ (pH 6.2 ± 0.1) to yield DPs. Next, a solution of plain emulsion particles was diluted to the same particle density ($1.3 \times 10^{10} \text{ cm}^{-3}$) in the buffer to give APs. The SHG measurements were carried out using an 800 nm fundamental beam. The 400 nm SHG signal was detected at 90° with respect to the incident beam (see the SI). The SHG signal of DPs in a quartz cuvette was monitored for ~ 10 min to ensure adsorption equilibrium. Figure 2 shows that for $t < 0$, the DPs generated a stable SHG signal, which was normalized to 1. At $t = 0$, an equal volume of APs at the same particle density was rapidly injected into the DP solution. The signal immediately dropped to ~ 0.5 . Next, for $t > 0$, I_{SHG} decayed because of the transfer of SPs from DPs to APs. As $t \rightarrow \infty$, I_{SHG} reached ~ 0.25 , where a new equilibrium was established and the SP molecules were equally distributed onto DPs and APs. Figure 2 a–c shows different signal-to-noise levels due to different integration times per data point: 5.0 s for MG-octyl-1, 0.5 s for MG-butyl-1, and 0.2 s for MG, which were adjusted because of the duration of the measurements.

The I_{SHG} decays as shown in Figure 2 were fitted to eq 4 to obtain the transfer rate constants k . Each measurement was repeated at least three times to yield the average k values (7.3 ± 0.2) $\times 10^{-5} \text{ s}^{-1}$ for MG-octyl-1, (5.2 ± 1.6) $\times 10^{-2} \text{ s}^{-1}$ for MG-butyl-1, and $0.24 \pm 0.03 \text{ s}^{-1}$ for MG. Decreasing the alkyl chain length from eight to four carbons led to an increase in the rate by a factor of ~ 600 . Further shortening the chain from butyl to methyl increased the rate by a factor of ~ 5 . The results suggest that for longer alkyl chains, the transfer rate is lower. Because we carried out all of the SHG measurements under the same conditions, the different rates are due to the structural variations in the alkyl chain. Thus, our results reveal that the hydrophobic interactions between the surfactant's alkyl chains and the oil phase play an important role in the rate-determining step of the transfer process.

To ensure that the emulsion system was stable upon addition of SPs and during the SHG experiments, we monitored the UV–vis spectra of the DPs and APs. Figure 1b shows UV–vis spectra of DPs bearing MG-octyl-1 and plain APs. The AP spectrum is due to Rayleigh scattering. The DP spectrum shows the UV–vis adsorption of SPs on top of the scattering background, suggesting that the emulsion was stable upon addition of MG-octyl-1. The DP and AP spectra were the same

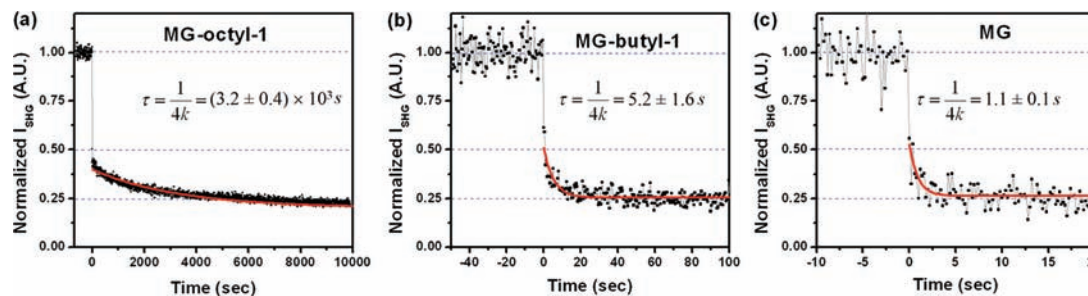


Figure 2. Time-dependent SHG intensities for (a) MG-octyl-1, (b) MG-butyl-1, and (c) MG. The data points are shown as dots, and the red lines are fits to eq 4. Each measurement was repeated at least three times, and the average decay times are shown as $(3.2 \pm 0.4) \times 10^3 \text{ s}$ for MG-octyl-1, $5.2 \pm 1.6 \text{ s}$ for MG-butyl-1, and $1.1 \pm 0.1 \text{ s}$ for MG.

before and after the SHG measurements, indicating that the emulsions were stable during the SHG experiments. Similar results for MG-butyl-1 and MG are given in the SI.

When we derived the equations to analyze the kinetic data, we assumed the concentration of free SP in the bulk solution to be negligible relative to the surface population. We verified this assumption by measuring the adsorption isotherm (see the SI). The total SP concentration used in the kinetic measurements was 2.3 μM for $t < 0$, which became 1.2 μM for $t > 0$. The adsorption isotherms (see the SI) confirmed that 2.3 and 1.2 μM were below the adsorption saturation. From the adsorption isotherm, we estimate that <1% of the total SP was free in solution, validating our assumption (see the SI). Indeed, Figure 2 shows excellent agreement between the measured and theoretical I_{SHG} values (1, 0.5, and 0.25 for $t < 0$, $t = 0$, and $t \rightarrow \infty$, respectively), further verifying the assumption.

The synthetic method used in this study is versatile and can be used to create a wide range of SPs with varying properties. The method couples the MG headgroup to one or two alkyl chains via the Buchwald–Hartwig reaction.¹² Hence, it is possible to use variety of secondary amines that can contain linear, branched, or cyclic aliphatic or aromatic hydrocarbon chains and are commercially available or accessible by reported synthetic procedures. Access to structurally diverse SP molecules is expected to be useful for studying the effect of carbon chains on surfactant transfer between colloidal emulsion particles, yielding practical information for optimizing emulsion systems and developing new detergent molecules.

Because of a lack of techniques, the transfer kinetics of surfactant molecules in emulsion systems has remained largely unexplored. The methodology developed here allows surfactant molecule transfer between emulsion particles to be probed in situ and in real time. This is expected to be useful for studying mechanisms of surfactant transfer between emulsion droplets and investigating various factors controlling the kinetics. Besides the effect of the alkyl chain, the method could also probe the effects of the physical and chemical environments (e.g., temperature, pH, electrolyte concentration, and surface potential) on the transfer rate.

Although our synthetic method is limited to detergent molecules with the MG headgroup, the coherent nature of the SHG signal could be used to probe detergent molecule transfer between colloidal emulsion particles in other molecular systems. In fact, the fundamental beam is not limited to the output from a Ti:Sapphire laser (~ 800 nm), and other light sources (e.g., in the visible region) could also be used. Hence, the SHG method can be applied to other detergent molecules, as long as the headgroups have UV–vis absorptions in resonance with the fundamental or SH wavelength.

To conclude, we have found that the four extra carbons on MG-octyl-1 (**3**) slow the transfer process relative to MG-butyl-1 (**2**) by a factor of 600. Our studies provide the first experimental method to study surfactant molecule transfer between colloidal emulsion droplets in situ and in real time. Our synthesis of the SP molecules **2** and **3** is straightforward and should allow versatile structural modifications of the carbon chain of the surfactants. Collectively, we expect that our approach of combining SHG spectroscopy with SP synthesis will enable further investigations of the mechanism and energetics of the transfer process, which are currently difficult to study using conventional methods. Hence, our method can be used to examine molecular mechanisms of detergent transfer, including exchange of oil phase, collision of detergent

particles, or desorption–adsorption of detergent molecules. The SHG method can be readily applied to measure the activation energy of the transfer process.¹⁸ The approach will also allow investigations of various factors controlling the kinetics, yielding useful information for optimizing compositions and conditions of emulsion systems for better performance in their industrial and environmental remediation applications.

■ ASSOCIATED CONTENT

📄 Supporting Information

Experimental procedures, characterization data, adsorption isotherms, and UV–vis spectral data. This material is available free of charge via the Internet at <http://pubs.acs.org>.

■ AUTHOR INFORMATION

Corresponding Author

seth.herzon@yale.edu; elsa.yan@yale.edu

Author Contributions

[†]These authors contributed equally.

Notes

The authors declare no competing financial interest.

■ ACKNOWLEDGMENTS

We thank Prof. M. Elimelech and Dr. Z. Meng (Yale University) for their help with the DLS measurements. This work was supported by ACS PRF (49557-DNIS to E.C.Y.Y.) and the Yale University Setup Fund (to S.B.H.). J.L. was the recipient of the Anderson Postdoctoral Fellowship.

■ REFERENCES

- (1) *Emulsions: Fundamentals and Applications in the Petroleum Industry*; Schramm, L. L., Ed.; Advances in Chemistry Series, Vol. 231; American Chemical Society: Washington, DC, 1992.
- (2) Sjoblom, J.; Aske, N.; Auflem, I. H.; Brandal, O.; Havre, T. E.; Saether, O.; Westvik, A.; Johnsen, E. E.; Kallevik, H. *Adv. Colloid Interface Sci.* **2003**, *100*, 399.
- (3) Chern, C. S. *Prog. Polym. Sci.* **2006**, *31*, 443.
- (4) Dimitratos, J.; Elicabe, G.; Georgakis, C. *AIChE J.* **1994**, *40*, 1993.
- (5) Nielloud, F.; Marti-Mestres, G. *Pharmaceutical Emulsions and Suspensions*; Marcel Dekker: New York, 2000.
- (6) Stumm, W.; Morgan, J. J. *Aquatic Chemistry*, 3rd ed.; Wiley: New York, 1996.
- (7) Kaminski, W.; Kwapinski, W. *Pol. J. Environ. Stud.* **2000**, *9*, 37.
- (8) Reed, M.; Johansen, O.; Brandvik, P. J.; Daling, P.; Lewis, A.; Fiocco, R.; Mackay, D.; Prentki, R. *Spill Sci. Technol. Bull.* **1999**, *5*, 3.
- (9) Fanun, M. *Microemulsions: Properties and Applications*; CRC Press: Boca Raton, FL, 2009.
- (10) (a) Malassagne-Bulgarelli, N.; McGrath, K. M. *Soft Matter* **2009**, *5*, 4804. (b) Kabalnov, A. J. *Dispersion Sci. Technol.* **2001**, *22*, 1.
- (11) Anna, S. L.; Alvarez, N. J.; Lee, W.; Walker, L. M. *J. Colloid Interface Sci.* **2011**, *355*, 231.
- (12) (a) Wolfe, J. P.; Wagaw, S.; Buchwald, S. L. *J. Am. Chem. Soc.* **1996**, *118*, 7215. (b) Stambuli, J. P.; Kuwano, R.; Hartwig, J. F. *Angew. Chem., Int. Ed.* **2002**, *41*, 4746.
- (13) (a) Shen, Y. R. *Annu. Rev. Phys. Chem.* **1989**, *40*, 327. (b) Shen, Y. R. *Nature* **1989**, *337*, 519. (c) Shen, Y. R. *The Principles of Nonlinear Optics*; Wiley: New York, 1984. (d) Eisenthal, K. B. *Chem. Rev.* **1996**, *96*, 1343. (e) Eisenthal, K. B. *Chem. Rev.* **2006**, *106*, 1462. (f) Corn, R. M.; Higgins, D. A. *Chem. Rev.* **1994**, *94*, 107. (g) Bloembergen, N.; Pershan, P. *Phys. Rev.* **1962**, *128*, 606.
- (14) (a) Conboy, J. C.; Daschbach, J. L.; Richmond, G. L. *J. Phys. Chem.* **1994**, *98*, 9688. (b) Gragson, D. E.; Richmond, G. L. *J. Phys. Chem. B* **1998**, *102*, 569. (c) Moore, F. G.; Richmond, G. L. *Acc. Chem. Res.* **2008**, *41*, 739. (d) Wang, H.; Borguet, E.; Yan, E. C. Y.; Zhang,

D.; Gutow, J.; Eienthal, K. B. *Langmuir* **1998**, *14*, 1472. (e) Paul, H. J.; Corn, R. M. *J. Phys. Chem. B* **1997**, *101*, 4494. (f) Naujok, R. R.; Paul, H. J.; Corn, R. M. *J. Phys. Chem.* **1996**, *100*, 10497. (g) Hommel, E. L.; Allen, H. C. *Analyst* **2003**, *128*, 750.

(15) (a) Roke, S.; Roeterdink, W. G.; Wijnhoven, J.; Petukhov, A. V.; Kleyn, A. W.; Bonn, M. *Phys. Rev. Lett.* **2003**, *91*, No. 258302. (b) Dadap, J. I.; de Aguiar, H. B.; Roke, S. *J. Chem. Phys.* **2009**, *130*, No. 214710. (c) Campen, R. K.; Pymmer, A. K.; Nihonyanagi, S.; Borguet, E. *J. Phys. Chem. C* **2010**, *114*, 18465. (d) Schneider, L.; Schmid, H.; Peukert, W. *Appl. Phys. B: Lasers Opt.* **2007**, *87*, 333. (e) Wang, H.; Yan, E. C. Y.; Borguet, E.; Eienthal, K. B. *Chem. Phys. Lett.* **1996**, *259*, 15. (f) Wang, H. F.; Yan, E. C. Y.; Liu, Y.; Eienthal, K. B. *J. Phys. Chem. B* **1998**, *102*, 4446. (g) Eckenrode, H. M.; Jen, S. H.; Han, J.; Yeh, A. G.; Dai, H. L. *J. Phys. Chem. B* **2005**, *109*, 4646. (h) Yang, N.; Angerer, W.; Yodh, A. *Phys. Rev. Lett.* **2001**, *87*, No. 103902. (i) Campen, R. K.; Zheng, D. S.; Wang, H. F.; Borguet, E. *J. Phys. Chem. C* **2007**, *111*, 8805. (j) de Beer, A. G. F.; de Aguiar, H. B.; Nijssen, J. F. W.; Roke, S. *Phys. Rev. Lett.* **2009**, *102*, No. 095502. (k) Wang, H. F.; Troxler, T.; Yeh, A. G.; Dai, H. L. *J. Phys. Chem. C* **2007**, *111*, 8708. (l) Boutou, V.; Favre, C.; Woeste, L.; Wolf, J. *Opt. Lett.* **2005**, *30*, 759. (m) de Aguiar, H. B.; de Beer, A. G. F.; Strader, M. L.; Roke, S. *J. Am. Chem. Soc.* **2010**, *132*, 2122. (n) de Aguiar, H. B.; Strader, M. L.; de Beer, A. G. F.; Roke, S. *J. Phys. Chem. B* **2011**, *115*, 2970. (o) Yan, E. C. Y.; Eienthal, K. B. *J. Phys. Chem. B* **1999**, *103*, 6056. (p) Srivastava, A.; Eienthal, K. B. *Chem. Phys. Lett.* **1998**, *292*, 345. (q) Yan, E. C. Y.; Eienthal, K. B. *Biophys. J.* **2000**, *79*, 898. (r) Liu, J.; Shang, X. M.; Pompano, R.; Eienthal, K. B. *Faraday Discuss.* **2005**, *129*, 291.

(16) (a) Dadap, J. I.; Shan, J.; Eienthal, K. B.; Heinz, T. F. *Phys. Rev. Lett.* **1999**, *83*, 4045. (b) Dadap, J. I.; Shan, J.; Heinz, T. F. *J. Opt. Soc. Am. B* **2004**, *21*, 1328. (c) de Beer, A. G. F.; Roke, S. *Phys. Rev. B* **2009**, *79*, No. 155420. (d) Jen, S. H.; Gonella, G.; Dai, H. L. *J. Phys. Chem. A* **2009**, *113*, 4758. (e) Jen, S.-H.; Dai, H.-L.; Gonella, G. *J. Phys. Chem. C* **2010**, *114*, 4302.

(17) Yan, E. C. Y.; Liu, Y.; Eienthal, K. B. *J. Phys. Chem. B* **2001**, *105*, 8531.

(18) Gan, W.; Xu, B. L.; Dai, H. L. *Angew. Chem., Int. Ed.* **2011**, *50*, 6622.